

This is an author-created, un-copyedited version of an article accepted for publication in Smart Materials and Structures. IOP Publishing Ltd is not responsible for any errors or omissions in this version of the manuscript or any version derived from it. The definitive publisher-authenticated version is available online at doi:10.1088/0964-1726/20/10/105013

S Boisseau et al 2011 Smart Mater. Struct. 20 105013
<http://iopscience.iop.org/0964-1726/20/10/105013>

Cantilever-based electret energy harvesters

S Boisseau¹, G Despesse¹, T Ricart¹, E Defay¹ and A Sylvestre²

¹CEA/LETI, 17 avenue des martyrs, Minatec Campus, Grenoble, France

²G2ELab, CNRS, 25 avenue des Martyrs, Grenoble, France

E-mail: sboisseau@gmail.com

Abstract. Integration of structures and functions has permitted to reduce electric consumptions of sensors, actuators and electronic devices. Therefore, it is now possible to imagine low-consumption devices able to harvest energy in their surrounding environment. One way to proceed is to develop converters able to turn mechanical energy, such as vibrations, into electricity: this paper focuses on electrostatic converters using electrets. We develop an accurate analytical model of a simple but efficient cantilever-based electret energy harvester. Therefore, we prove that with vibrations of 0.1g ($\sim 1\text{m/s}^2$), it is theoretically possible to harvest up to $30\mu\text{W}$ per gram of mobile mass. This power corresponds to the maximum output power of a resonant energy harvester according to the model of William and Yates. Simulations results are validated by experimental measurements, raising at the same time the large impact of parasitic capacitances on the output power. Therefore, we ‘only’ managed to harvest $10\mu\text{W}$ per gram of mobile mass, but according to our factor of merit, this puts us in the best results of the state of the art.

1. Introduction

Thanks to size reduction, micro-electro-mechanical-systems (*MEMS*) are consuming less and less energy, giving them the opportunity to harvest energy in their surrounding environment. This field of research called ‘Energy Harvesting’ consists in the development of converters able to turn ambient energy (light, air flux, variation of temperatures, vibrations) into electricity that is used to power the microsystem. Many principles of conversion have already been developed: photovoltaic, thermoelectric, biofuelcells... As for mechanical energy from vibrations, it can be converted by three main different principles: piezoelectric, electromagnetic and electrostatic conversion. In this study, we focus on electrostatic converters which are based on a capacitive architecture (two charged electrodes spaced by an air gap) and connected to a load. Vibrations induce changes in the geometry of the capacitor and a circulation of charges between electrodes through the electrical load. The electronic circuit that manages power conversion of ‘standard’ electrostatic energy harvesters [1] is quite complicated and induces losses and therefore a decrease of efficiency. To limit the use of a management electronic circuit, it is possible to use electrets (stable electrically charged dielectrics) that polarize the capacitance and allow to harvest energy from vibrations without using cycles of charging and discharging.

Many electret-based energy harvesters have been developed and have proven the interest of such devices [2-22]. Most of these devices are in-plane structures where the variation of capacitance is obtained by a variation of surface between patterned electrodes, while the gap is kept constant. These structures are generally hard to manufacture using elaborate clean room processes and especially DRIE (Deep Reactive Ion Etching) but give the opportunity to harvest energy when the vibrations of the ambient environment are not constant because they avoid contacts between electrets and electrodes. In this paper, we have chosen to study a simpler structure: the ‘cantilever-based electret

energy harvester'. This structure does not maximize the output power of the energy harvester if vibrations are not well defined but is particularly suitable when vibrations are stable in terms of frequency and amplitude in the time. Moreover, this structure is quite easy to manufacture and therefore low-cost.

In section 2, we present the theory of vibration energy harvesting and more especially of energy harvesting using electrets. Then, we develop an accurate analytical model, its implementation (under Matlab/Simulink) and its validation using FEM (Finite Element Method). Thanks to this model, the structure can be optimized, as presented in section 4. Finally, in section 5, we present experimental results and a comparison to simulation results. We finally develop a model taking parasitic capacitances into account to explain the differences between our first model and experimental results.

2. Electret-based energy harvesters using cantilevers

Our electret-based energy harvester is a microsystem able to convert mechanical energy from vibrations into electricity. It is part of vibration energy harvesters whose general model is presented hereafter.

2.1. William and Yates' general model for vibration energy harvesters

Regardless of the conversion principle (electrostatic, electromagnetic or piezoelectric), resonant energy harvesters can be modeled as a mobile mass (m) suspended to a support by a spring (k) and damped by forces (f_{elec} and f_{mec}). When a vibration occurs $y(t) = Y \sin(\omega t)$, it induces a relative displacement of the mobile mass $x(t) = X \sin(\omega t + \varphi)$ compared to the frame (figure 1). Part of the kinetic energy of the moving mass is lost due to mechanical damping (f_{mec}) while the other part is converted into electricity, which is modeled by an electrostatic force (f_{elec}) in electrostatic energy harvesters. Ambient vibrations are generally low in amplitude (typically $Y=25\mu\text{m}$) and the use of a mass-spring structure enables to take advantage of a resonance phenomenon that amplifies the amplitude of vibrations perceived by the mobile mass and the harvested energy. Newton's second law gives the differential equation that rules the movement of the mobile mass (1).

$$m\ddot{x} + kx + f_{elec} + f_{mec} = -m\ddot{y} \quad (1)$$

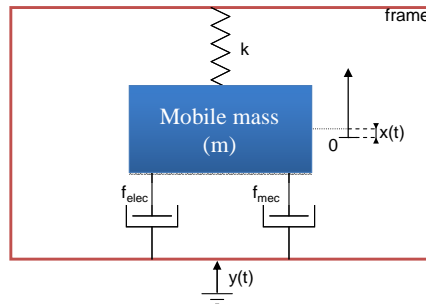


Figure 1. Mechanical system.

When forces can be modeled as viscous forces, $f_{elec} = b_e \dot{x}$ and $f_{mec} = b_m \dot{x}$, where b_e and b_m are respectively electrical and mechanical damping coefficients, William and Yates [23] have proven that the maximum output power of a resonant energy harvester subjected to an ambient vibration is reached when the natural angular frequency (ω_n) of the mass-spring structure is tuned to the angular frequency of ambient vibrations (ω) and when the damping rate $\xi_e = b_e / (2m\omega_n)$ of the electrostatic force f_{elec} is equal to the damping rate $\xi_m = b_m / (2m\omega_n)$ of the mechanical friction force f_{mec} . This maximum output power $P_{W\&Y}$ can be simply expressed with (2), when $\xi_e = \xi_m = \xi$.

$$P_{W\&Y} = \frac{mY^2\omega_n^3}{16\zeta} \quad (2)$$

As $P_{W\&Y}$ is a good approximation to know the output power of vibration energy harvesters when forces are modeled as viscous forces, comparing the output power (P) of a resonant energy harvester to $P_{W\&Y}$ gives a legitimate factor of merit $\alpha_{W\&Y}$:

$$\alpha_{W\&Y} = \frac{P}{P_{W\&Y}} \quad (3)$$

Nevertheless, in many studies, the weight of the mobile mass is not given while the surface area of the electrodes (S) is often provided. Therefore, to compare systems, we had developed, in a previous study, an other factor of merit, normalized by the active surface S in place of the mass [24]:

$$\chi = \frac{P}{Y^2\omega^3S} \quad (4)$$

These two factors of merit will be used in the next parts, to compare our system to the state of the art.

2.2. Cantilever-based electret energy harvesters – Principles and Model

The particularity of electret-based energy harvesters is the use of an electret to maintain the electrostatic converter charged through time. Electrets are dielectrics able to keep an electric field (and a surface voltage V) for years thanks to charge trapping (figure 2). These materials are in electrostatics, the equivalent to magnets in magnetostatics.

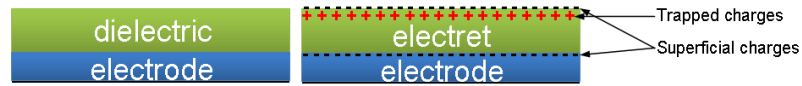


Figure 2. Electret film.

Electrets are obtained by implanting electric charges into dielectrics. Theoretically, dielectrics do not conduct electricity; therefore, the implanted charges stay trapped inside. Many techniques exist to manufacture electrets [25, 26], but the most common is the corona discharge (figure 3). It consists in a point-grid-plane structure whose point is subjected to a strong electric field: it leads to the creation of a plasma, made of ions. These ions are projected onto the surface of the sample to charge, and transfer their charges to its surface (figure 2), into the bulk or at the interfaces of the material. The grid is used to limit the surface voltage of the electret to a wanted final value.

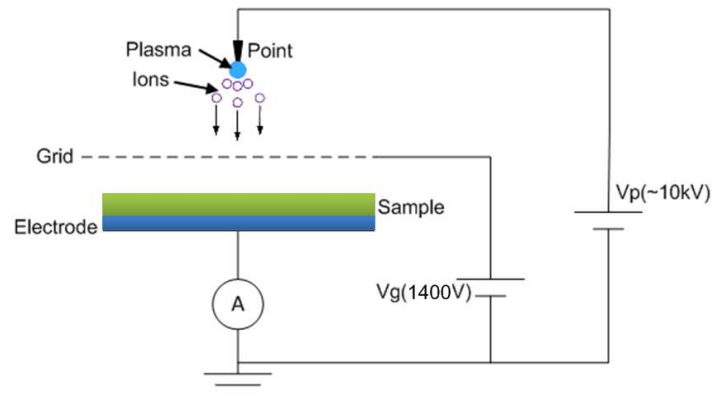


Figure 3. Corona discharge used to charge our device.

Nevertheless, dielectrics are not perfect insulators and implanted charges can move inside the material or can be compensated by other charges or environmental conditions, and finally disappear. A focal area of research on electrets concerns their stability [15, 27, 28]. Nowadays, many materials are

known as good electrets able to keep their charges for years: for example, Teflon® and silicon dioxide (SiO₂) whose stability is estimated to more than 100 years [29-32].

The structure able to turn vibrations into electricity using electrets is introduced in figure 4: the system is composed of a counter-electrode and an electrode on which is deposited an electret, spaced by an air gap and connected by an electrical load (here a resistor). The electret has a constant charge Q_i , and, due to electrostatic induction and charges conservation, the sum of charges on the electrode and on the counter-electrode equals the charge on the electret: $Q_i = Q_1 + Q_2$.

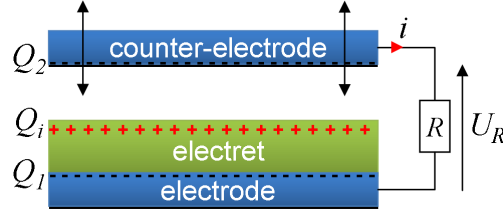


Figure 4. Electrostatic converter using electret.

When a vibration occurs, it induces a change in the capacitor geometry (e.g. the counter-electrode moves away from the electret, changing the air gap and then the electret influence on the counter-electrode) and a reorganization of charges between the electrode and the counter-electrode through the load. This induces a current across the load R and part of the mechanical energy is then turned into electricity.

The converter introduced in figure 4 is integrated into a clamped-free beam mechanical structure (figure 5). The lower face of the beam is metalized and is used as the counter-electrode. The electret and the electrode are placed under the beam, separated by an air gap and electrically connected by a load (figure 5(a)). According to William and Yates' formula (2), the output power is proportional to the mobile mass; consequently, to increase the output power, a proof mass m is added at the free end of the cantilever. Vibrations $y(t)$ induce a relative displacement $x(t)$ of the mobile mass compared to the electrode. Structure parameters are presented in figure 5(b): h is the beam thickness, w its width, L the length between the clamping and the gravity center of the mass, $2L_m$ the mass length, $g(t)$ the thickness of the air gap between the counter-electrode and the electret, g_0 the thickness of this air gap without vibrations and without the weight effects \vec{W} , V the surface voltage of the electret, C_1 the capacitance of the electret, C_2 the capacitance of the air gap and finally λ the electrode length.

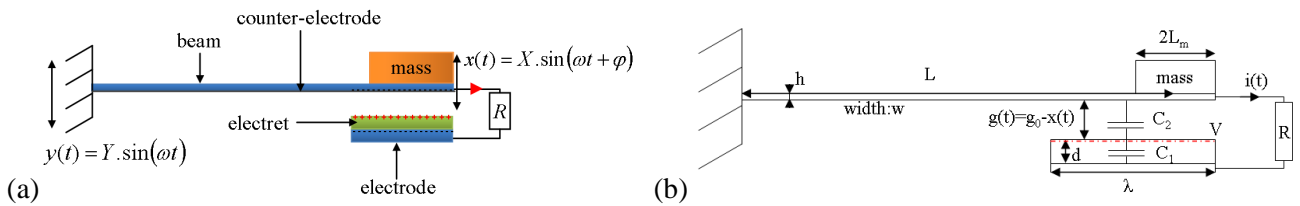


Figure 5. (a) Cantilever-based energy harvester using electrets. (b) Energy harvester parameters.

To identify the main parameters of this kind of energy harvesters and to maximize the output power for a given vibration ($y(t) = Y \cdot \sin(\omega t)$), it is necessary to find coupled mechanical and electrostatic equations that rule the energy harvester.

3. Analytical model of the ‘Cantilever-based electret energy harvester’

To determine the output power of the energy harvester for a given vibration $y(t)$, it is necessary to solve the equation of motion and to find the quantity of charge transferred to the output. Therefore, the goal of section 3 is to develop the analytical model of the ‘cantilever-based electret energy harvester’ parameterized in figure 5 for mechanical and electrostatic parts.

3.1. Model of the mechanical system

The clamped-free beam with a mass at the free end can be modeled as a damped mass-spring structure as presented in figure 1 and by adding the effect of weight $\vec{W} = m\vec{g}$. The mechanical friction

forces can be modeled as viscous forces ($f_{mec} = b_m \dot{x}$) and the electrostatic force is the derivative of the electrostatic energy of the capacitor W_e with respect to the displacement x . W_e is equal to the charge on the upper electrode Q_2 squared, divided by two times the capacitance as a function of time $C(t)$. Thereby, the mechanical system is ruled by (5).

$$m\ddot{x} + b_m \dot{x} + kx - \frac{d}{dx}(W_e) - mg = -m\ddot{y} \Rightarrow m\ddot{x} + b_m \dot{x} + kx - \frac{d}{dx} \left(\frac{Q_2^2}{2C(t)} \right) - mg = -m\ddot{y} \quad (5)$$

To maximize the output power of the energy harvester, the natural angular frequency ($\omega_n = \sqrt{k/m}$) of the mass-spring structure has to be tuned to the angular frequency of the ambient vibrations (ω). Moreover, according to equations from mechanical structures theory, the spring constant k can be deduced from the beam geometric parameters as follow:

$$k = m\omega_n^2 = \frac{3EI}{L^3} = \frac{Ewh^3}{4L^3} \quad (6)$$

Where E is the Young's modulus and I the quadratic moment of the beam.

Because of the mass, the behavior of the beam has to be studied on two parts. A drawing of the structure is presented in figure 6 and shows the deformation of the cantilever $\delta(z)$ as a function of the position on the cantilever z for a forced deflection x at $z=L$. The first part ($z \in [0, L_1 = L - L_m]$) does not have an additional mass: its behavior corresponds to the one of a clamped-free beam whose deflection at the end (x_1) is imposed and given by $\delta(z) = \frac{x_1}{2L_1^3} z^2 (3L_1 - z)$. The second part that has the additional mass ($z \in [L_1, L_2 = L + L_m]$) follows the deflection of part 1: the derivative of the deflection ($\delta(z)$) with respect to the position (z) for part 2 is constant and equal to the derivative of the deflection of part 1 at $z=L_1$ (7).

$$c = \left. \frac{d\delta(z)}{dz} \right|_{z=L_1} = \left. \frac{d\delta(z)}{dz} \right|_{z \in [L_1, L_2]} = \frac{3}{2} \frac{x_1}{L_1} \text{ with } x_1 = x - cL_m \quad (7)$$

Therefore, for a given static deflection (x) on the position L of the beam, the deformation of the beam can be simply expressed as a function of the parameters in both parts:

$$\begin{cases} \delta(z) = \frac{x_1}{2L_1^3} z^2 (3L_1 - z) & [\text{part 1}] \\ \delta(z) = c(z - L) + x & [\text{part 2}] \end{cases} \quad (8)$$

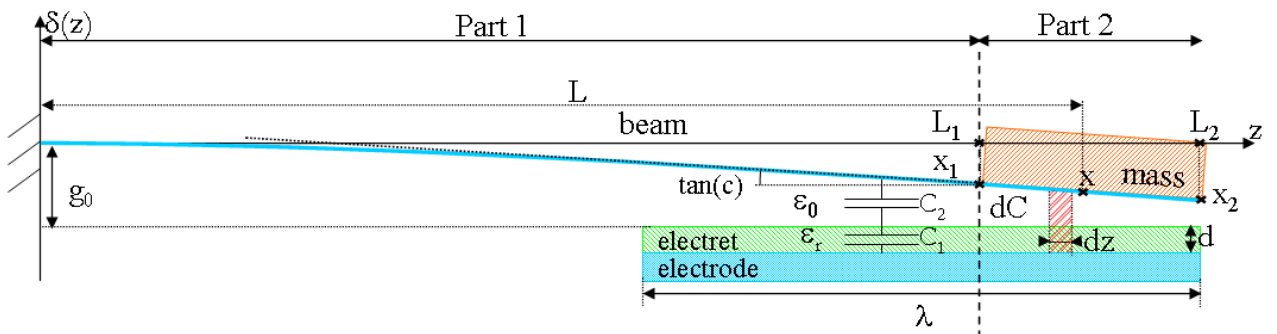


Figure 6. Deformation of the cantilever for an imposed deflection (x).

Figure 7 presents the beam deformation resulting from equation (8) for a beam of $L=30\text{mm}$ and $L_m=2\text{mm}$ and for an imposed static displacement of $x=300\mu\text{m}$ compared to the deformation performed by FEM calculation (Comsol® Multiphysics). It proves that our calculations fit with FEM results.

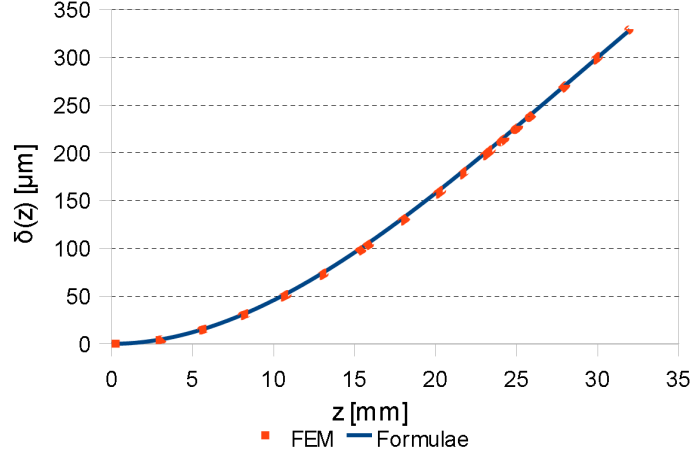


Figure 7. Deformation of the cantilever for an imposed static deflection (x).

Nevertheless, the problem we want to solve is not static but dynamic. Therefore, it is useful to verify that the beam deformation behavior is the same in dynamic and in static. We have verified this using FEM : it confirms that the deformation in dynamic and in static can be considered as equivalent. Thus, we can consider that the deflection in dynamics can be simply expressed with (8) assuming that x is the imposed deflection on the mass gravity point.

3.2. Modeling of the electrostatic system

The equivalent model of the energy harvester is presented in figure 8, where Q_2 is the charge on the counter-electrode, V the surface voltage of the electret and $C(t)$ the capacitance between the beam and the electrode. This capacitance corresponds to the serial capacitance formed by the electret dielectric material capacitance C_1 and the air gap capacitance $C_2(t)$. Kirchoff's laws give the differential equation that governs the electrostatic system (9):

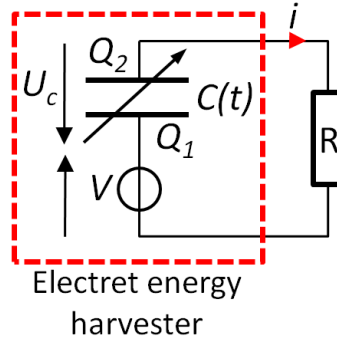


Figure 8. Equivalent electric model of the energy harvester.

$$\frac{dQ_2}{dt} = \frac{V}{R} - \frac{Q_2}{R} \times \left[\frac{1}{C(t)} \right] = \frac{V}{R} - \frac{Q_2}{R} \times \left[\frac{1}{C_1} + \frac{1}{C_2(t)} \right] \quad (9)$$

Moreover, the electrostatic energy stored in the capacitor is:

$$W_e = \frac{1}{2} \frac{Q_2^2(t)}{C(t)} \quad (10)$$

To solve (9), it is necessary to know the capacitance of the electrostatic converter as a function of the imposed deflection (x). Knowing the cantilever deformation, and considering a capacitor of infinitesimal length (dz) (figure 6), one can get the infinitesimal capacitance on both part (dC_{p1} and dC_{p2}) for a given x .

$$\left\{ \begin{array}{l} dC_{p_1}(x) = \frac{\varepsilon_0 w dz}{g_0 - \delta(z) + \frac{d}{\varepsilon_r}} \text{ with } \delta(z) = \frac{x_1}{2L_1^3} z^2 (3L_1 - z) \text{ [part 1]} \\ dC_{p_2}(x) = \frac{\varepsilon_0 w dz}{g_0 - \delta(z) + \frac{d}{\varepsilon_r}} \text{ with } \delta(z) = c(z - L) + x \text{ [part 2]} \end{array} \right. \quad (11)$$

By integrating these expressions, the total capacitance between both electrodes is:

$$C(x) = C_{p_1}(x) + C_{p_2}(x) = \varepsilon_0 w \int_{L_2 - \lambda}^{L_1} \frac{dz}{g_0 - x \frac{z^2 (3L - z)}{2L^3} + \frac{d}{\varepsilon_r}} + \frac{\varepsilon_0 w}{c} \ln \left(\frac{g_0 + \frac{d}{\varepsilon_r} + cL_m - x}{g_0 + \frac{d}{\varepsilon_r} - cL_m - x} \right) \quad (12)$$

The integral defining $C_{p_1}(x)$ cannot be analytically calculated and will be numerically computed.

This capacitance expression has been compared to a FEM simulation and the curves presented in figure 9 show that results are in excellent agreement. These results were also compared to the formula of a simple plane capacitor neglecting fringe effects ($C(x) = \varepsilon_0 S / (g_0 - x + d / \varepsilon_r)$), where S is the surface of the electrodes, g_0 the initial gap and x the imposed deflection. With our parameters ($L_m=2\text{mm}$, $L=30\text{mm}$, $g_0=505\mu\text{m}$, $d=100\mu\text{m}$, $w=12.33\text{mm}$, $\varepsilon_r=2$, $\lambda=10\text{mm}$), we have found that the model of the simple plane capacitor overestimate (up to 35%) the maximal capacitance of the energy harvester.

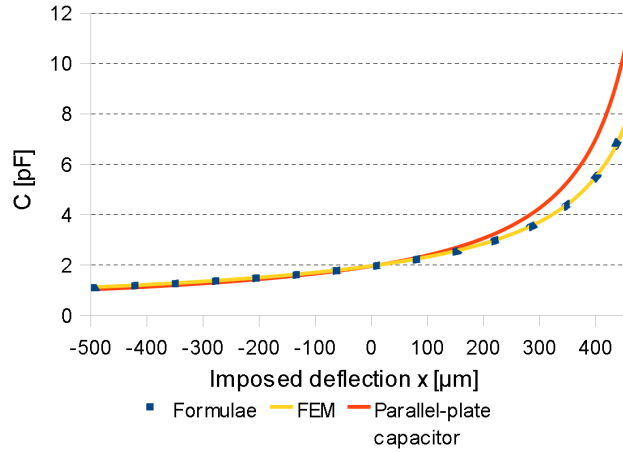


Figure 9. Capacitance between the electrodes (C) versus forced displacement (x) ($L_m=2\text{mm}$, $L=30\text{mm}$, $g_0=505\mu\text{m}$, $d=100\mu\text{m}$, $w=12.33\text{mm}$, $\varepsilon_r=2$, $\lambda=10\text{mm}$).

This accurate value of the capacitance for a given deflection is then applied in the mechanical system introduced in section 3.1.

3.3. Complete analytical model

In order to get the output power of the energy harvester, mechanical and electrostatic systems have to be coupled. From (5) and (9), one can find that the system of equations that governs the energy harvester is (13).

$$\left\{ \begin{array}{l} m\ddot{x} + b_m \dot{x} + kx - \frac{d}{dx} \left(\frac{Q_2^2}{2C(t)} \right) - mg = -m\ddot{y} \\ \frac{dQ_2}{dt} = \frac{V}{R} - \frac{Q_2}{C(t)R} \end{array} \right. \quad (13)$$

Nevertheless, it is not possible to get an analytic expression of x and Q_2 . Therefore, the system is numerically solved in Matlab/Simulink (figure 10).

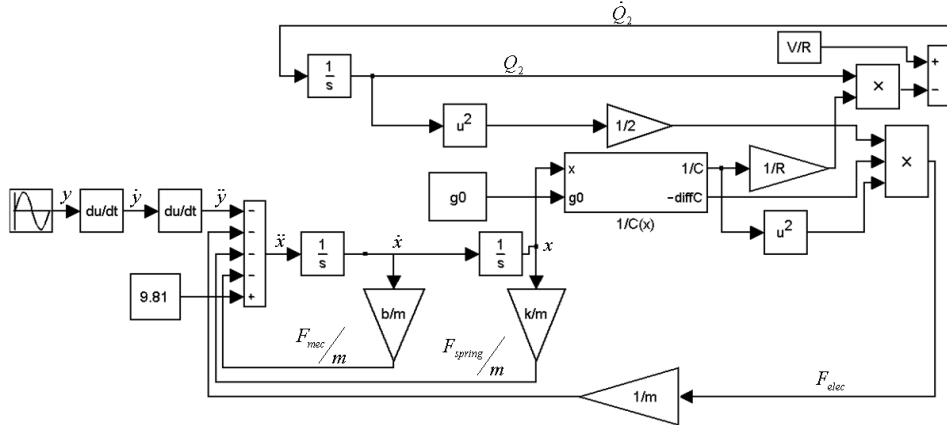


Figure 10. Simulink model of the energy harvester.

The deflection (x) given by Matlab and the voltage across the resistor $U_R = R(dQ_2/dt)$ versus time are presented in figure 11(a) and 11(b) for $V=1400V$, $d=127\mu m$, $g_0=1mm$, $\lambda=20mm$, $R=300M\Omega$.

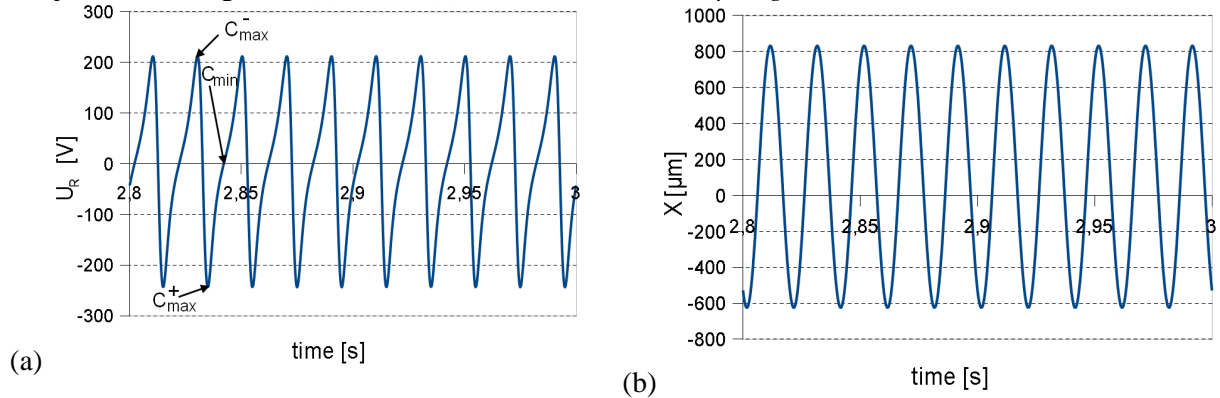


Figure 11. (a) Example of output voltage and (b) deflection versus time.

Figure 11(a) shows that the output voltage of ‘cantilever-based electret energy harvesters’ can be higher than 200V. This can greatly simplify rectification of the output voltage using diode bridges. Moreover, figure 11(a) shows a particularity of the output voltage of cantilever-based electret energy harvesters: output voltage presents a discontinuity when it passes from its higher value (the capacitance is just before its maximum C_{max}^-) to its lower value (the capacitance is just after its maximum C_{max}^+) because the current changes direction when the capacitance crosses its maximum. The current also changes direction when the capacitance crosses its minimum C_{min} . But, since the output voltage equals 0 when the capacitance is minimum, no discontinuity on the output voltage appears.

In section 3, we have developed the complete analytical model of the energy harvester and its implementation on Simulink. Thanks to this model, the system can be optimized to give the maximum output power.

4. Output power and Optimization

The goal of this section is to maximize the average output power of the energy harvester P for a given vibration $y(t)$. Actually, the power can be simply computed from the derivative of Q_2 given by the Simulink model presented in figure 10 (14). We will determine in section 4.1 the parameters to optimize before optimizing them in section 4.2.

$$P = \frac{1}{t_2 - t_1} \int_{t_1}^{t_2} R \left(\frac{dQ_2}{dt} \right)^2 dt \text{ where } t_1 \text{ and } t_2 \text{ are times taken in the steady state} \quad (14)$$

4.1. Parameters to optimize

We have chosen to consider L , L_m , m , w , k , Y , $\omega=2\pi f$, V , ϵ_r , d and ζ as given parameters and the load R , the electrode length λ and the initial air gap g_0 as parameters to optimize. Figures 12(a), 12(b) and 12(c) present the output power of the energy harvester when one parameter varies while the other are kept constant. Constant values are: $Y=10\mu\text{m}$, $f=50\text{Hz}$, $m=5\text{g}$, $\zeta=1/150$, $V=1400$, $w=12.3\text{mm}$, $d=127\mu\text{m}$, $\epsilon_r=2$, $L_m=2\text{mm}$, $L=30\text{mm}$ and $R=1\text{G}\Omega$, $\lambda=10\text{mm}$, $g_0=2\text{mm}$ when one of them varies.

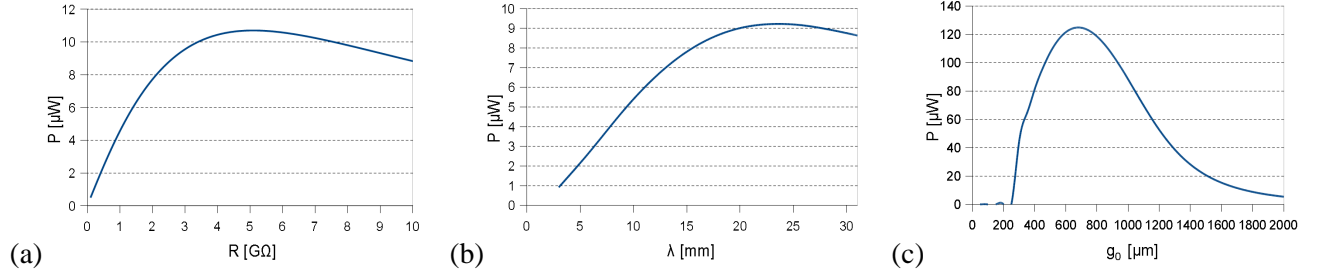


Figure 12. Parameters to optimize and their effect on the average output power: (a) load, (b) length of the electrode and (c) initial gap.

It is obvious that those three parameters play an important role in the behavior of the energy harvester and it is also obvious that an optimum is present in each curve signifying that optimal parameters exist. As these parameters are not independent, they have to be optimized together in a single loop.

4.2. Optimization and maximum output power

The optimization process uses the *fminsearch* Matlab function to minimize the inverse of the output power ($1/P$) considering (R , λ and g_0) as parameters. Table 1 gives the maximum output powers and the optimal parameters for different mobile masses for an ‘ambient’ vibration of $(Y, f)=(10\mu\text{m}, 50\text{Hz})\approx 1\text{ms}^{-2}$: it proves that the model of William and Yates gives a good approximation of the output power but is not rigorously exact in ‘cantilever-based electret energy harvesters’. Actually, if the system could be modeled by William and Yates model, $\alpha_{w\&y}$ should be equal to 1 whatever the value of the mobile mass. Moreover, when the electrostatic force is sufficiently high, which is directly linked to the surface voltage of the electret, output power of the energy harvester is bigger than the output power determined by William and Yates’ model. When the surface voltage of the electret is not high enough to induce a sufficient electrostatic force that can absorb the kinetic energy of the mobile mass, it cannot permit to obtain the optimal energy with the mobile mass (e.g. when $m=10\text{g}$). For $m=5\text{g}$, a surface voltage of 1400V should allow to harvest $160\mu\text{W}$ which corresponds to a power density per mass unit of $\sim 30\mu\text{W/g}$.

Table 1. Output Power (P) as a function of the mass (m) with $V=1400\text{V}$.

m (g)	R_{opt} (G Ω)	λ_{opt} (mm)	g_{0opt} (μm)	P (μW)	$P_{w\&y}$ (μW)	P/m ($\mu\text{W/g}$)	$\alpha_{w\&y}$
1	10	6.4	700	36.59	29.07	36.59	1.26
2	7.1	5.9	602	71.7	58.14	35.85	1.23
3	4.36	7.4	600	104	87.21	34.67	1.19
5	2.18	9.6	593	160	145.34	32	1.1
10	0.8	14.30	901	173	290.68	17.3	0.6

The results presented in table 1 are given with an accuracy of $1\mu\text{m}$ for g_0 and $10\mu\text{m}$ for λ . These precisions will not be easy to obtain. To see the effect of inaccuracies on λ and g_0 on the response of the system, we have plotted the output power of the system when g_0 and λ range from $100\mu\text{m}$ to their optimal values (0 corresponds to the optimal value). Results presented in figure 13 prove that the output power does not vary much near the optimal values of g_0 and λ , but to avoid a contact between

the counter-electrode and the electret, for the prototype, we will choose a value of g_0 slightly higher than the optimal value. Therefore, even with inaccuracies on λ and g_0 ($\sim 50\mu\text{m}$), the output power should be equal to at least $140\mu\text{W}$.

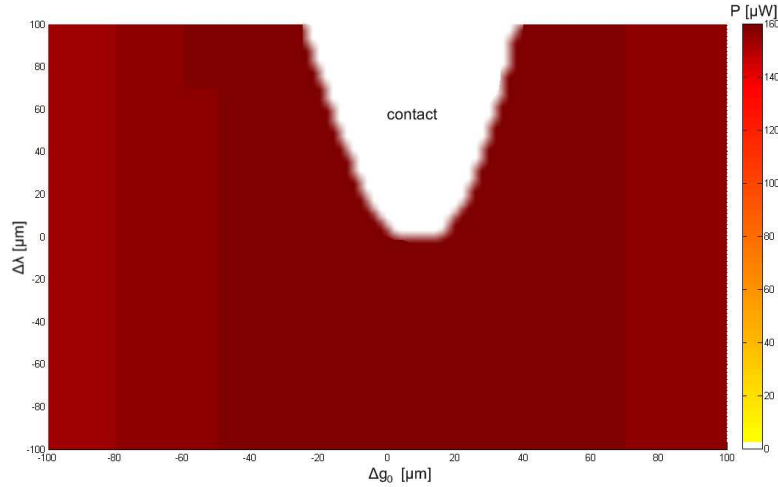


Figure 13. Output power in function of λ and g_0 variations around their optimal value.

Similarly, the effect of the frequency and the amplitude of vibrations were evaluated on the optimal design. As the system is resonant and low damped, f and Y variations induce a large output power change (figure 14): these parameters are critical but can be adjusted with a good accuracy. Therefore, it proves that, when the parameters of vibrations are constant, cantilever-based electret energy harvesters are good energy harvesters. But, if the amplitude of vibrations increases, it can lead to a contact between the upper electrode and the electret that can damage this latter.

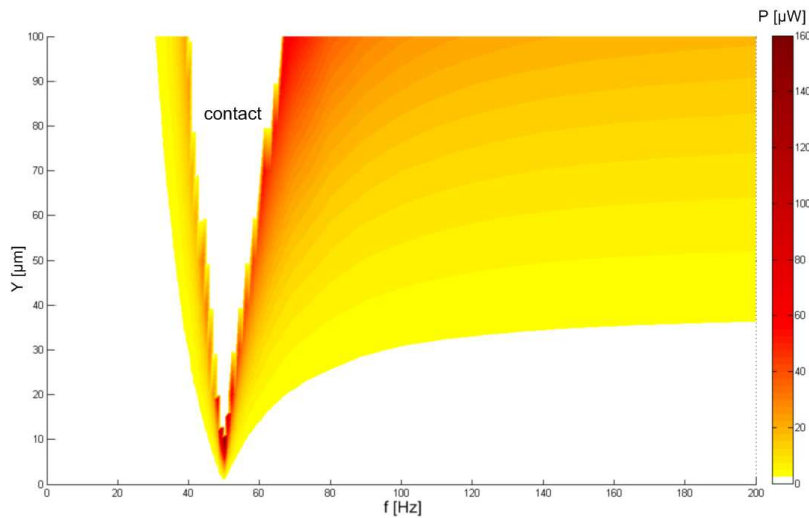


Figure 14. Effect of the vibrations on the optimized system.

The resonant system has been optimized and theoretical results have proven that up to $160\mu\text{W}$ could be reached with low vibrations ($10\mu\text{m}@50\text{Hz}$) $\approx 1\text{ms}^{-2}$. These parameters are now tested on a prototype.

5. Experimental results and new model taking parasitic capacitances into account

The goal of experimental results presented in section 5 is to validate theoretical results that have been obtained in the previous sections and to see the limits of our model. We conclude this section with a better analytical model of the energy harvester that takes parasitic capacitances into account.

5.1. Prototype and expected output power

To insure a good flatness, the beam is made in silicon and attached to the frame at one end. The mobile mass attached to the other end is made in tungsten that has a high density ($d=17$) to limit its size. The electret is made in Teflon FEP (Fluorinated Ethylene Propylene) that is well known for being a good electret [32]. In this study, the electret is charged to 1400V. Our prototype design is presented in figure 15.

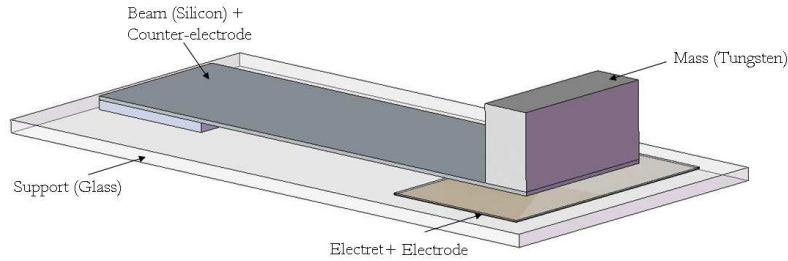


Figure 15. Cantilever-based electret energy harvester – Schema.

The natural frequency of the structure, computed with FEM, is actually 48.77Hz. The difference with our model is due to the simplification in (6). To fit the vibrations imposed by the environment (50Hz), the beam width is slightly changed to 13mm. Therefore, the output power of the energy harvester should be $140\mu\text{W}$ and the voltage across the resistance versus time should look like the one presented on figure 16(a) given by simulation (figure 16(b) is a zoom of figure 16(a)).

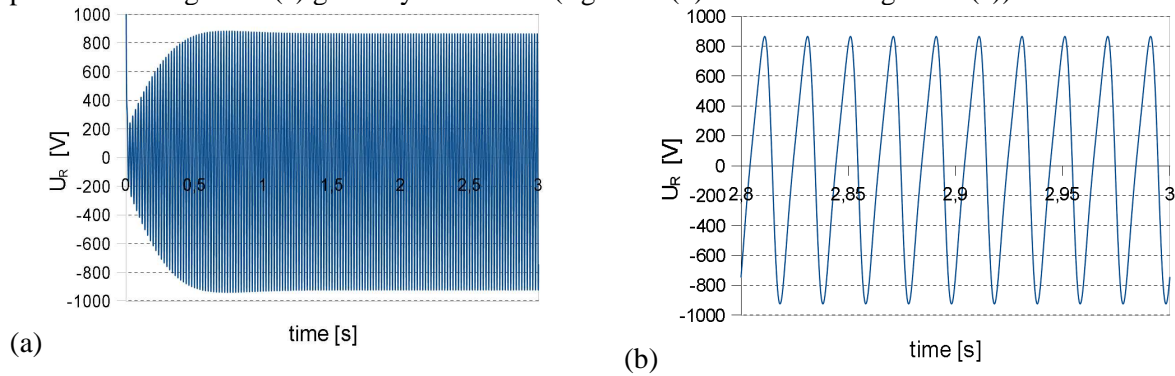


Figure 16. (a) Output voltage of the energy harvester versus time. (b) Zoom of figure 15(a) ($m=5\text{g}$, $V=1400\text{V}$, $R=2.18\text{G}\Omega$, $\lambda=9.6\text{mm}$, $g_0=593\mu\text{m}$, $Y=10\mu\text{m}$, $f=50\text{Hz}$).

The prototype was made on a glass support (figure 17(a)) to limit parasitic capacitances. A mass of 5g in tungsten was added at the free end of the cantilever. The electret is obtained by evaporating a 300nm-thick layer of aluminum on the rear face of a Teflon FEP film. It is glued on a sheet of copper to ensure the flatness of the electret during charging. The electret is charged using a standard corona discharge as presented in figure 3 with a point voltage V_p of 10kV and a grid voltage V_g of 1400V. It is placed in an oven at 175°C and cooled to the ambient temperature while charging to improve stability. The long-term stability was not studied but the short-term (some days) experiments showed low charge losses (-0.21% in 8 days) (figure 17(b)).

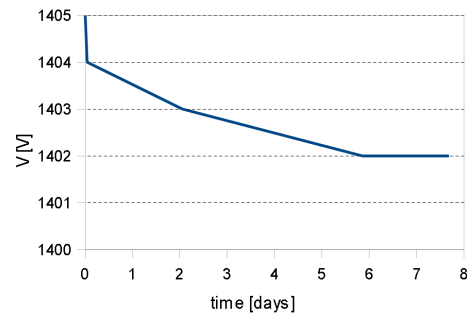
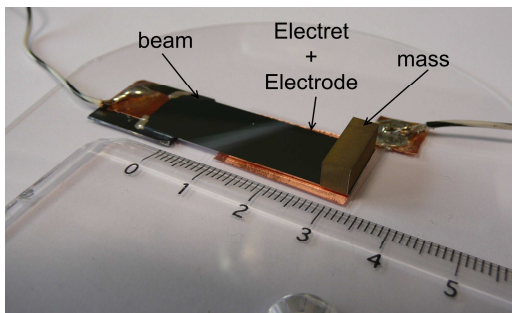


Figure 17. (a) Cantilever-based electret energy harvester – prototype. (b) Stability of Teflon FEP electret charged at 1400V

5.2. Output Power, comparison to the theory and limits

We present hereafter the experimental results we got on our prototype. The optimized parameters were applied to the prototype introduced in figure 17(a). The output power of our prototype is presented in figure 18(a). Experimental and theoretical curves do not fit and the output power is much lower than expected. These differences are due to parasitic capacitances that become important when using loads of high values. In those cases, the model given in figures 5(b) and 8 should be modified to take a parasitic capacitance C_{par} in parallel with the load into account.

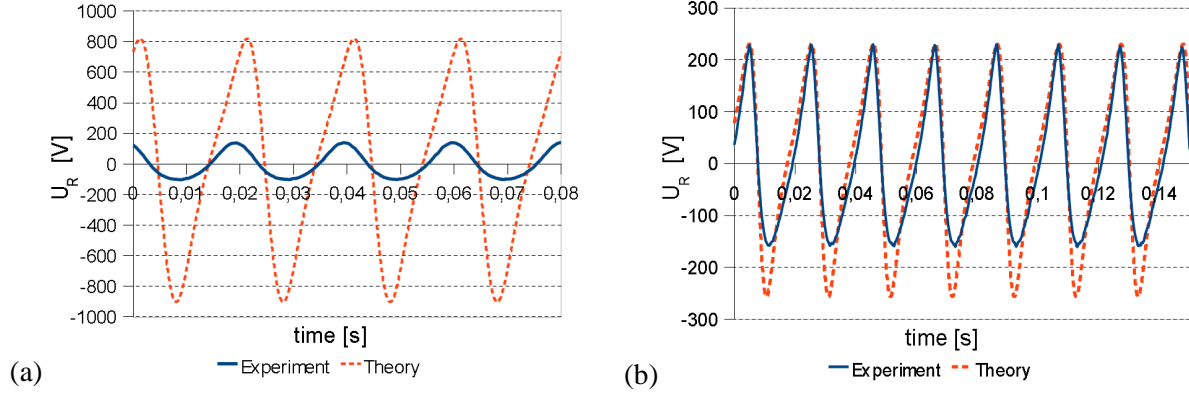


Figure 18. Experimental output voltages (a) for $R=2,2G\Omega$ and (b) for $R=300M\Omega$.

To avoid these phenomena, the value of the load was constraint to $300M\Omega$ (chosen after some experimental measurements in order to limit the parasitic capacitances induced by the load) and the optimization process was restarted on g_0 and λ . ‘New’ optimized values are presented in table 2.

Table 2. Parameters and values.

Parameter	Designation	Value
M_{beam}	Material of the beam	Silicon
E	Young’s Modulus of Silicon	160 GPa
L	distance between the clamping and the centre of gravity of the mass	30 mm
h	Thickness of the beam	300 μm
w	Width of the beam / Width of the electret	13 mm
$2Lm$	Length of the mobile mass	4 mm
m	Mobile mass	5 g
$\omega_n = \omega$	Natural angular frequency/Angular frequency of vibrations	$50 \times 2\pi$ rad/s
$Q_m = (2\xi_m)^{-1}$	Mechanical quality factor of the structure	75
$M_{electret}$	Material of the electret	FEP
ϵ_r	Dielectric constant of the electret	2
d	Thickness of the electret	127 μm
V	Surface voltage of the electret	1400 V
g_0	Thickness of the initial air gap	700 μm
λ	Length of the electrode	22.8 mm
R	Load	300 $M\Omega$

The structure was tested again with the new load and its output voltage is presented in figure 18(b). Experimental and theoretical curves fit, except for negative voltages. This is once again due to parasitic capacitances that clip the signal in its negative part. The mean output power of the energy harvester is $50\mu\text{W}$ when it is submitted to vibrations of $10\mu\text{m}@50\text{Hz}$ (1ms^{-2}) (our simulation predicted $80\mu\text{W}$).

Table 3. Comparison to 7 prototypes among the most recent electret energy harvesters in the state of the art.

Author	Ref	Vibrations	Active Surface (S)	Electret Potential (V)	Output Power (P)	Figure of merit (χ)
Suzuki	[14]	1mm@37Hz (54.0ms ⁻²)	2.33 cm ²	450V	0.28μW	9.56×10 ⁻⁵
Halvorsen	[16]	2.8μm@596Hz (39.2ms ⁻²)	0.48 cm ²		1μW	5.06×10 ⁻²
Kloub	[17]	0.08μm@1740Hz (9.6ms ⁻²)	0.42 cm ²	25V	5μW	14.2
Naruse	[18]	25mm@2Hz (3.9ms ⁻²)	9 cm ²		40μW	3.58×10 ⁻²
Edamoto	[19]	500μm@21Hz (8.7ms ⁻²)	3 cm ²	600 V	12μW	6.97×10 ⁻²
Miki	[20]	100μm@63Hz (15.7ms ⁻²)	3 cm ²	180V	1μW	5.37×10 ⁻³
Honzumi	[21]	9.35μm@500Hz (92ms ⁻²)	0.01 cm ²	52V	90 pW	3.32×10 ⁻⁵
This work (th.)		10μm@50Hz (1.0ms ⁻²)	4.16cm ²	1400V	152μW	117.84
This work (exp.)		10μm@50Hz (1.0ms ⁻²)	4.16cm ²	1400V	50μW	38.75

Our experimental results correspond to a factor of merit $\alpha_{w\&y}$ equals to 34% and to a factor of merit χ equals to 38.75, putting us in the best results of the state of the art (table 3), yet, our experimental results are quite different from theoretical results.

5.3. Model taking parasitic capacitances into account

In order to explain the differences between our theory and our experimental results, we have developed a new model that takes parasitic capacitances into account. The parasitic capacitance of the whole system is modeled as a capacitor C_{par} in parallel with the energy harvester and the load, as presented in figure 19. U is the voltage across the resistor, the parasitic capacitance and the electret energy harvester.

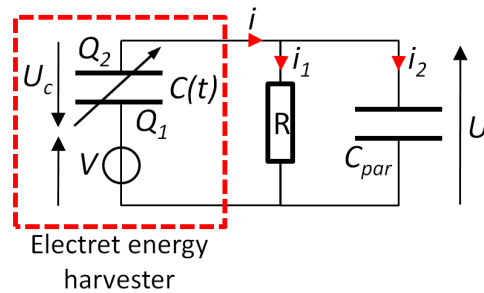


Figure 19. Equivalent electric model of the energy harvester taking parasitic capacitance into account.

In order to model the behavior of the energy harvester taking parasitic capacitances into account, the equation that rules the electrostatic part is modified as follow (15) (obtained using Kirchoff's laws) while the equation that rules the mechanical part is the same as in (5) and (13).

$$\frac{dQ_2}{dt} = \frac{1}{\left(1 + \frac{C_{par}}{C(t)}\right)} \left(\frac{V}{R} - Q_2 \left(\frac{1}{RC(t)} - \frac{C_{par}}{C(t)^2} \frac{dC(t)}{dt} \right) \right) \quad (15)$$

And the instantaneous harvested power is given by (16):

$$p(t) = \frac{U^2}{R} = \frac{1}{R} \left(V - \frac{Q_2}{C(t)} \right)^2 \quad (16)$$

Our Simulink model was modified to take these changes into account. Our experimental results were then compared to our theoretical results taking parasitic capacitances into account (figures 20(a) and 20(b)) where parasitic capacitances with the 300MΩ load are estimated to 5pF and to 10pF with the 2.2GΩ load.

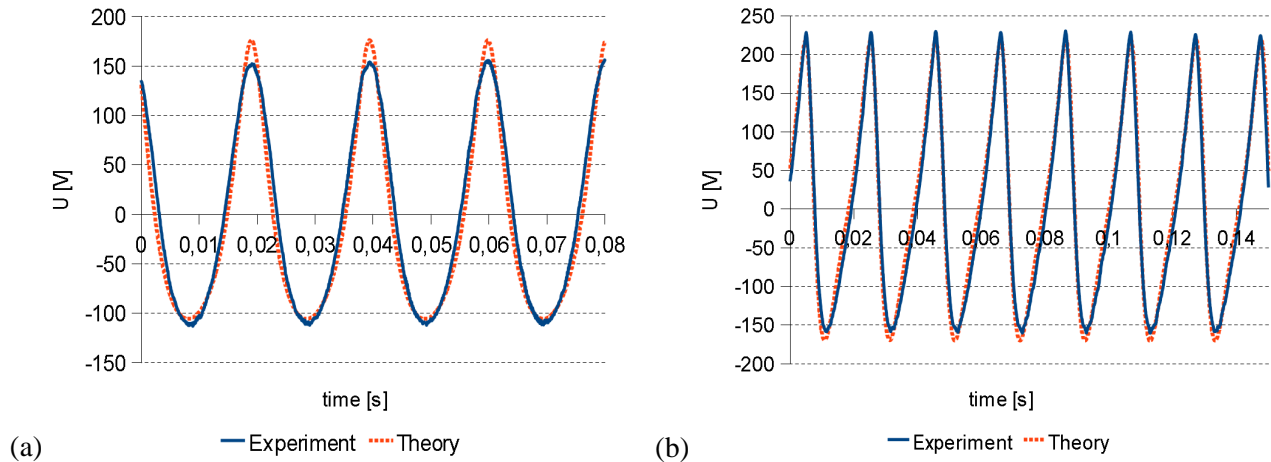


Figure 20. Experimental output voltages (a) for $R=2,2G\Omega$ and (b) for $R=300M\Omega$ and comparison to theory taking parasitic capacitances into account.

Figures 20(a) and 20(b) show that theoretical and experimental results fit perfectly and validate our new model. Therefore, it appears that parasitic capacitances have a large impact on the behavior of the energy harvester, decreasing the harvested power, especially when using high-value resistors. Unfortunately, as parasitic capacitances greatly depend on the load, restarting an optimization process taking parasitic capacitances into account would be difficult. Moreover, it would have a limited interest since parasitic capacitances can change a lot with the use of management electronic circuits. Therefore, to limit their effects, the load should be chosen so as not to exceed $Z_{par} = \frac{1}{C_{par}\omega}$, the impedance of the parasitic capacitances which is roughly equal to $Z_{par}=500M\Omega$ in our case.

6. Conclusion and perspectives

We developed an analytical model of ‘cantilever-based electret energy harvester’ that is in agreement with FEM results. The optimization process has shown that the power harvested by these structures are in the same magnitude as theoretical output powers developed by William and Yates as soon as the surface voltage of the electret is sufficient to absorb the kinetic energy of the mobile mass. Finally, we validated our model with experimental results which reach up to $10\mu W$ per gram of mobile mass for low ambient vibrations of $0.1g$ ($1ms^{-2}$), using a resonant system.

Cantilever-based energy harvester can be a good low-cost solution to harvest energy when vibrations are constant in frequency and amplitude. The output power meets the magnitude of powers reached by piezoelectric or electromagnetic solutions.

References

- [1] Despesse G *et al.* 2005 High damping electrostatic system for vibration energy scavenging *Proc. Joint sOc-EUSAI conference* pp 283-6
- [2] Tada Y 1992 Experimental characteristics of electret generator using polymer film electrets *Japan. J. Appl. Phys.* **31** pp 846–51
- [3] Genda T, Tanaka S and Esashi M 2003 High power electrostatic motor and generator using electrets *Proc. Transducers '03* pp 492–5
- [4] Boland J S, Messenger J D M, Lo H W and Tai Y C 2005 Arrayed liquid rotor electret power generator systems *Proc. MEMS'05* pp 618–21
- [5] Peano F and Tambosso T 2005 Design and optimization of a MEMS electret-based capacitive energy scavenger *Journal of MEMS* **14** pp 429-35
- [6] Tsutsumino T, Suzuki Y, Kasagi N and Sakane Y 2006 Seismic power generator using high-performance polymer electret *Proc. MEMS'06* pp 98–101
- [7] Lo H-W, Whang R and Tai Y-C 2007 A simple micro electret power generator *Technical Digest MEMS2007* pp 859–62

- [8] Sterken T, Fiorini P, Altena G, Van Hoof C and Puers R 2007 Harvesting energy from vibrations by a micromachined electret generator *Int. Conf. Solid-State Sensors, Actuators and Microsystems* pp 129–32
- [9] Sterken T, Altena G, Fiorini P and Puers R 2007 Characterization of an electrostatic vibration harvester *DTIP of MEMS and MOEMS*
- [10] Tvedt L G W, Blystad L C J and Halvorsen E 2008 Simulation of an electrostatic energy harvester at large amplitude narrow and wide band vibrations *Symp. on DTIP of MEMS/MOEMS* pp 296-301
- [11] Lo H W and Tai Y C 2008 Parylene-HT-based electret rotor generator *Proc. MEMS'08* pp 984–7
- [12] Zhang J and Lv Z 2008 A fruit jelly mems electret power generator *Proc. PowerMEMS'08* pp 285–8
- [13] Yang Z, Wang J and Zhang J 2008 A micro power generator using PECVD SiO₂/Si₃N₄ double-layer as electret *Proc. PowerMEMS'08* pp 317–20
- [14] Suzuki Y, Edamoto M, Kasagi N, Kashwagi K and Morizawa Y 2008 Micro electrets energy harvesting device with analogue impedance conversion circuit *Proc. PowerMEMS'08* pp 7–10
- [15] Sakane Y *et al.* 2008 The development of a high-performance perfluorinated polymer electret and its application to micro power generation *J. Micromech. Microeng.* **18** 104011
- [16] Halvorsen E, Westby E R, Husa1 S, Vogl A, Østbø N P, Leonov V, Sterken T and Kvisterøy T 2009 An electrostatic Energy harvester with electret bias *Proc. Transducers'09* pp 1381–84
- [17] Kloub H, Hoffmann D, Folkmer B and Manoli Y 2009 A micro capacitive vibration Energy harvester for low power electronics *Proc. PowerMEMS'09* pp 165–8
- [18] Naruse Y, Matsubara N, Mabuchi K, Izumi M and Suzuki S 2009 Electrostatic micro power generation from low-frequency vibration such as human motion *Journal of Micromechanics and Microengineering* **19** 094002
- [19] Edamoto M *et al.* 2009 Low-resonant-frequency micro electret generator for energy harvesting application *Proc. MEMS'09* pp 1059–62
- [20] Miki D, Honzumi M, Suzuki Y and Kasagi N 2010 Large-amplitude MEMS electret generator with nonlinear spring *Proc. MEMS'2010* pp 176–9
- [21] Honzumi M *et al.* 2010 Soft-X-Ray-charged vertical electrets and its application to electrostatic transducers *Proc. MEMS'2010* pp 635–8
- [22] Yamashita K *et al.* 2010 Vibration-driven MEMS energy harvester with vertical electrets *Proc. PowerMEMS'2010* pp 165-8
- [23] Williams C B and Yates R B 1996 Analysis of a micro-electric generator for microsystems *Sensors Actuators A* **52** pp 8–11
- [24] Boisseau S, Despesse G and Sylvestre A 2010 Optimization of an electret-based energy harvester *Smart Materials and Structures* **19** 075015
- [25] Giacometti J A, Fedosov S and Costa M M 1999 Corona charging of polymers: recent advances on constant current charging *Brazilian Journal of Physics* **29** pp 269-79
- [26] Ikezaki K, Miki M and Tamura J I 1981 Thermally stimulated currents from ion-injected teflon-FEP film electrets *Japanese Journal of Applied Physics* **20** pp 1741-7
- [27] Honzumi M *et al.* 2010 High-speed electret charging method using vacuum UV irradiation *Proc. PowerMEMS'2010* pp 173-6
- [28] Chen Q 2002 PTFE electret negative charge stability after RF plasma treatment *J. Phys. D: Appl. Phys.* **35** 2939
- [29] Amjadi H 1999 Charge storage in double layers of thermally grown silicon dioxide and APCVD silicon nitride *IEEE Transactions on Dielectrics and Electrical Insulation* **6** pp 852-7
- [30] Leonov V, Fiorini P and Van Hoof C.U. 2006 Stabilization of positive charge in SiO₂/Si₃N₄ electrets *IEEE transactions on Dielectrics and Electrical Insulation* **13** pp 1049-56
- [31] Kressmann R, Sessler G and Gunther P 1996 Space-charge electrets *IEEE Transactions on Dielectrics and Electrical Insulation* **3** pp 607-23
- [32] Kotrappa P 2008 Long term stability of electrets used in electret ion chambers *Journal of Electrostatics* **66** pp 407-9